Eur. Phys. J. B **30**, 25–32 (2002)
DOI: 10.1140/epjb/e2002-00334-3

THE EUROPEAN PHYSICAL JOURNAL B

Crystal structure and magnetic ordering of $RNi_{10}Si_2$ compounds

W. Kockelmann[1,2,a], M. Hofmann[2,b], O. Moze[3], S.J. Kennedy[4], and K.H.J. Buschow[5]

[1] Mineralogisch-Petrologisches Institut, Universität Bonn, 53115 Bonn, Germany
[2] ISIS Facility, Rutherford Appleton Laboratory, Chilton, Didcot, OX11 0QX, UK
[3] INFM, Dipartimento di Fisica, Università di Modena e Reggio Emilia, Via Campi 213/a, 41100, Modena, Italy
[4] Australian Neutron Scattering Group, ANSTO, Lucas Heights, Menai, Australia
[5] Van-der-Waals-Zeeman Institute, University of Amsterdam, Valckenierstraat 65, 1018 XE Amsterdam, The Netherlands

Received 10 July 2002 / Received in final form 12 September 2002
Published online 29 October 2002 –

Abstract. The element distributions and the magnetic ordering behaviour of compounds $RNi_{10}Si_2$ (R = Tb, Dy, Ho, Er, Tm) have been studied by neutron powder diffraction down to temperatures of 1.6 K. The compounds crystallize in an ordered variant of the $ThMn_{12}$ structure type in the tetragonal space group P4/nmm. An ordered 1:1 distribution of Ni and Si on sites 4d and 4e, respectively, corresponds to a modulation vector [0, 0, 1] with respect to the space group I4/mmm of the $ThMn_{12}$ structure. $TbNi_{10}Si_2$ orders antiferromagnetically below $T_N = 4.5$ K with a magnetic propagation vector of [0, 0, 1/2]. The magnetic Tb moments, 8.97(2) μ_B/Tb atom at 1.6 K, are aligned along the c-axis. The Ni sites in $TbNi_{10}Si_2$ do not carry any ordered magnetic moments. The compounds with R = Dy, Ho, Er, and Tm are paramagnetic down to 1.6 K and 3.0 K, respectively.

PACS. 61.12.-q Neutron diffraction and scattering – 61.50.Ks Crystallographic aspects of phase transformations; pressure effects – 75.25.+z Spin arrangements in magnetically ordered materials (including neutron and spin-polarized electron studies, synchrotron-source X-ray scattering, etc.)

1 Introduction

Rare earth (R) ternary compounds of the type $RT_{12-x}M_x$, where T is a 3*d* transition metal such as Mn, Fe, Co, Ni and M is a stabilising element such as V, Ti, Al, Si, have been investigated in great detail by bulk and microscopic measurements [1,2]. The principle motive for the interest arises from the fact that some of the iron and cobalt rich compounds of the series are inexpensive potential candidates for permanent magnet materials [2], *e.g.* samarium compounds such as $SmFe_{10}Si_2$ and $SmFe_{10}V_2$ have sufficiently high magnetic ordering temperatures, saturation magnetizations and magneto-crystalline anisotropies [3]. Compounds with T = Ni have been investigated to a lesser extent since they do not order magnetically at ambient temperatures and are therefore of less interest for applications. The Ni compounds are nevertheless of importance since they allow for an investigation of the magnetic properties in the absence of the strong exchange interactions between R and 3*d* sublattices, which are naturally present in corresponding Fe and Co compounds. The rare earth single ion anisotropy of Ni compounds is not affected by strong molecular fields from the T sites, and studying these compounds may help to shed light on the role of the crystal field interactions in corresponding isostructural Fe and Co compounds. Moreover, Ni atoms can be used to dilute the 3*d* magnetic sublattices as it was performed for the series $YCo_{10-x}Ni_xSi_2$ for small [4] and high Ni content [5]. These latter compounds exhibit successively, ferromagnetic, spin glass and paramagnetic behaviour with increasing Ni content.

Compounds $RT_{12-x}M_x$ crystallize in the tetragonal $ThMn_{12}$-type structure in space group I4/mmm [6], the concentration range of the solid solution depending on the T and M elements. A truly vast amount of X-ray and neutron powder diffraction work has been devoted to studying the crystal and magnetic structures of the $ThMn_{12}$ compounds ([3,7–9] and references therein). A small number of experiments have been performed on single crystal specimen such as $DyFe_4Al_8$ and $HoFe_4Al_8$ [10] or YFe_4Al_8 [11]. The $ThMn_{12}$ compounds have a rather simple crystal structure with rare earth atoms always occupying the site 2a(0,0,0), *i.e.* the corners and centres of the tetragonal unit cell. The T and M atoms are distributed over one or more of the non-equivalent positions 8f(1/4, 1/4, 1/4), 8i(x, 0, 0) and 8j(x, 1/2, 0). The 8f and 8j sites form two interpenetrating tetragonal prisms with R atoms in the centre (Fig. 1a). The T and M atoms

[a] e-mail: W.Kockelmann@rl.ac.uk
[b] *Present address:* Technische Universität München, ZBE FRM-II, 85747 Garching, Germany.

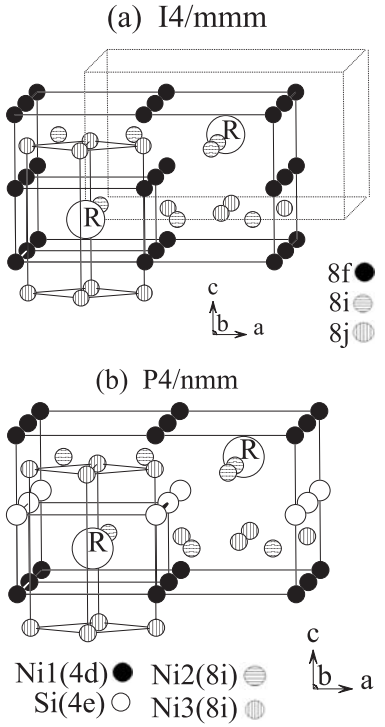

Fig. 1. Crystal structure. (a) $ThMn_{12}$ structure, I4/mmm, the origin being shifted by (1/4, 1/4, 1/4), the standard unit cell setting is indicated; (b) $RNi_{10}Si_2$ structure, P4/nmm.

generally show strong preferences for one or more of the three 8-fold sites. The actual occupation depends on the nature of the T and M elements, for example, a transition metal M = Ti, V in a T-rich compound shows preference for the 8i site whereas an s, p element M = Al, Si avoids and prefers the 8i site in a T-rich and M-rich compound, respectively [1]. It is worth mentioning that compositions RT_4M_8, *e.g.* RFe_4Al_8, allow for well ordered distributions of atoms on 8f, 8i, and 8j positions [8,9]. For compositions others than $x = 4$ and $x = 8$ perfectly ordered atomic distributions on the three symmetry sites cannot be achieved in the $ThMn_{12}$ structure, and the inevitable mixing of elements on equivalent symmetry positions strongly affects the magnetic properties of the compounds.

Rare earth 3d silicides crystallize in a small composition range around $x = 2$ only. A $ThMn_{12}$ structure is known to form only for the heavy rare earth series and for R = Y. High resolution neutron diffraction on $YNi_{10}Si_2$ confirmed crystallization in the $ThMn_{12}$ structure with $RNi_{11}Si_2$ ($NaZn_{13}$-type structure, $Fm\bar{3}c$) identified as a secondary phase [12]. Silicon atoms in $YNi_{10}Si_2$ were found on all three non-rare earth sites, however with a strong preference for the 8f site. This agrees with X-ray diffraction results on $RFe_{10}Si_2$ with Si atoms occupying the 8f and 8j positions [3]. This site occupation preference was qualitatively explained by mixing enthalpy effects of R and Si whereas atomic size effects were ruled out. The enthalpy argument was based on the negative heat of mixing of R and Si, being relatively large and negative [3], and on the fact that the 8f and 8j are the sites with highest coordination offering largest contact to the rare earth atoms. The crystal field parameters of $RNi_{10}Si_2$ compounds could not be evaluated unambiguously from inelastic neutron scattering data [13] but the studies indicated relatively weak crystal field interactions with the overall splitting in the order of 70 K. Well defined magnetic transitions were observed for $ErNi_{10}Si_2$ but the low temperature transitions of compounds with R = Tb, Ho were not well resolved pointing to a complex level system. Magnetization and susceptibility data on $TmNi_{10}Si_2$ showed that the Ni sublattices can be considered as non-magnetic [14]. Macroscopic measurements on $YNi_{10}Si_2$ showed no phase transition in the temperature range 4.2–300 K thus indicating that this compound is paramagnetic in the observed temperature range [5]. This further indicates that the Ni sublattices in $RNi_{10}Si_2$ compounds do not order magnetically in the absence of ordered rare earth magnetic moments.

In order to determine the element distributions and the magnetic ordering behaviour in the series $RNi_{10}Si_2$ we performed powder neutron diffraction measurements between 1.6 and 293 K for the heavy rare earth elements R = Tb, Dy, Ho, Er and Tm. The determination of the element distributions of these compounds is facilitated by a strong contrast in the neutron scattering lengths of Ni and Si.

2 Experimental

Samples with a nominal composition of $RNi_{10}Si_2$ were prepared by arc melting elemental raw materials of at least 3N purity in argon atmosphere. The resulting ingots, each of about 10 grams weight, were annealed at 1050 °C for 3 days in argon atmosphere. X-ray diffraction with Cu-K_α radiation confirmed that the prepared compounds crystallized in a tetragonal space group, tentatively assigned to I4/mmm whereas extra reflections were initially attributed to an impurity phase. As will be discussed in detail below, the prepared compounds actually crystallized in a subgroup of I4/mmm and are single phase.

Neutron diffraction measurements on $RNi_{10}Si_2$ (R = Dy, Ho, Er) were performed down to 1.6 K on the angle dispersive E9 powder diffractometer, located at the Hahn-Meitner Institute, Berlin, Germany. For this experiment, an incident neutron wavelength of 1.7963 Å was used. Data were collected in a 2θ-scattering angle range between 5 and 160 degrees. Energy dispersive time-of-flight (TOF) neutron diffraction data on $TbNi_{10}Si_2$ between 1.6–300 K and on $TmNi_{10}Si_2$ between 3–300 K were collected on ROTAX and POLARIS, respectively, located at the neutron spallation source ISIS at the Rutherford Appleton Laboratory, United Kingdom. Both TOF diffractometers are equipped with 3 detector banks, each of which provides neutron diffraction data in a distinct d-spacing and resolution range. These data complemented room temperature data taken earlier on $ErNi_{10}Si_2$ on the MRPD neutron diffractometer, located at the HIFAR research reactor, Lucas Heights, Australia, with an incident neutron wavelength of 1.6676 Å. Rietveld profile analyses of the diffraction patterns taken in angle-dispersive mode were performed using the program FullProf [15].

Table 1. Refined crystal structure parameters of $RNi_{10}Si_2$ compounds in the paramagnetic phase based on space group P4/nmm: lattice parameters a, c; atom positions y, z, shortest interatomic distance R-X to the rare earth position and isotropic temperature factors B. The Debye-Waller factors of the Dy compound were kept fixed at values obtained for the Tb compound. The weighted profile (R_{wp}) and nuclear Bragg (R_B) Rietveld reliability factors are given as criteria for the goodness of fits. Parameters in [*italics*] are based on refinements in space group I4/mmm. Estimated standard deviations are given in parentheses.

$TbNi_{10}Si_2$	T=25 K	a = 8.1965(1) Å	c = 4.6671(1) Å	R_{wp}= 2.6 %	R_B= 2.3 %	
	y/a		z/c	R-X [Å]		B (Å^2)
Tb (2c)	¼		0.2255(4) [*0.25*]			0.25(2)
Ni_1 (4d)	0		0 [*0*]	3.0832(6)	[*3.1242*]	0.36(2)
Si (4e)	0		½ [*½*]	3.1684(7)	[*3.1242*]	0.35(4)
Ni_2 (8i)	0.60426(6)	[*0.6040*]	0.2379(2) [*0.25*]	2.9042(5)	[*2.9016*]	0.35(1)
Ni_3 (8i)	0.02543(7)	[*0.0257*]	0.7298(2) [*0.75*]	2.9566(2)	[*2.9710*]	0.36(1)
$DyNi_{10}Si_2$	T=1.6 K	a = 8.18315(7) Å	c = 4.65954(6) Å	R_{wp}= 20.5 %	R_B= 7.3 %	
	y/a		z/c	R-X [Å]		B (Å^2)
Dy (2c)	¼		0.2306(11) [*0.25*]			0.25
Ni_1 (4d)	0		0 [*0*]	3.086(2)	[*3.119*]	0.35
Si (4e)	0		½ [*½*]	3.154(2)	[*3.119*]	0.35
Ni_2 (8i)	0.6036(3)	[*0.6040*]	0.2386(9) [*0.25*]	2.894(3)	[*2.897*]	0.35
Ni_3 (8i)	0.0257(3)	[*0.0255*]	0.7276(9) [*0.75*]	2.955(6)	[*2.967*]	0.35
$HoNi_{10}Si_2$	T=1.6 K	a = 8.17628(5) Å	c = 4.65744(4) Å	R_{wp}= 14.2 %	R_B= 6.7 %	
	y/a		z/c	R-X [Å]		B (Å^2)
Ho (2c)	¼		0.2356(16) [*0.25*]			0.30(7)
Ni_1 (4d)	0		0 [*0*]	3.092(3)	[*3.117*]	0.43(6)
Si (4e)	0		½ [*½*]	3.142(3)	[*3.117*]	0.27(13)
Ni_2 (8i)	0.6029(2)	[*0.6032*]	0.2373(7) [*0.25*]	2.886(2)	[*2.888*]	0.53(3)
Ni_3 (8i)	0.0276(2)	[*0.0277*]	0.7289(6) [*0.75*]	2.931(6)	[*2.955*]	0.46(4)
$ErNi_{10}Si_2$	T=1.6 K	a = 8.16766(3) Å	c = 4.65572(3) Å	R_{wp}= 11.5 %	R_B= 5.9 %	
	y/a		z/c	R-X [Å]		B (Å^2)
Er (2c)	¼		0.2280(12) [*0.25*]			0.42(6)
Ni_1 (4d)	0		0 [*0*]	3.077(2)	[*3.113*]	0.54(5)
Si (4e)	0		½ [*½*]	3.153(2)	[*3.113*]	0.25(10)
Ni_2 (8i)	0.6031(2)	[*0.6035*]	0.2386(5) [*0.25*]	2.885(2)	[*2.888*]	0.52(3)
Ni_3 (8i)	0.0279(2)	[*0.0280*]	0.7299(5) [*0.75*]	2.944(5)	[*2.951*]	0.43(3)
$TmNi_{10}Si_2$	T=3 K	a = 8.16799(5) Å	c = 4.65383(5) Å	R_{wp}= 2.1 %	R_B= 3.3 %	
	y/a		z/c	R-X [Å]		B (Å^2)
Tm (2a)	¼		0.2361(5) [*0.25*]			0.31(2)
Ni_1 (4d)	0		0 [*0*]	3.0895(9)	[*3.113*]	0.17(2)
Si_1 (4e)	0		½ [*½*]	3.138(1)	[*3.113*]	0.23(4)
Ni_2 (8i)	0.60361(6)	[*0.6033*]	0.2375(2) [*0.25*]	2.8882(5)	[*2.886*]	0.26(2)
Ni_3 (8i)	0.02824(7)	[*0.0286*]	0.7290(2) [*0.75*]	2.924(2)	[*2.947*]	0.19(2)

The time-of-flight data were analysed using the GSAS program [16]. The following neutron scattering lengths were used: $b_{Tb} = 7.38$ fm, $b_{Dy} = 16.9$ fm, $b_{Ho} = 8.01$ fm, $b_{Er} = 7.79$ fm, $b_{Tm} = 7.34$ fm, $b_{Ni} = 10.3$ fm and $b_{Si} = 4.15$ fm [17]. For the angle-dispersive data analysis Fullprof absorption parameter values of 1.2, 0.8, 0.5 for 'μR' for Dy, Ho, and Er, respectively, were used. For the time-of-flight data analysis a coefficient for a linear absorption as implemented in the GSAS program was refined.

3 Results and discussion

3.1 Crystal structure

The neutron diffraction patterns were firstly fitted using the $ThMn_{12}$ structure model based on space group I4/mmm (no 139), already proposed for the compound $YNi_{10}Si_2$ [12]. In this starting model R atoms were placed on the 2a site, whilst Ni and Si atoms were statistically distributed onto the 8f, 8i and 8j sites (Fig. 1a) according to stoichiometry. The best Rietveld fits for R = Tb, Dy, Ho, Er, Tm showed almost exclusive occupation of Si of the 8f positions, sharing them with Ni atoms. This strong site preference of Si for 8f agrees with the previous study on $YNi_{10}Si_2$ [12], although for the Y-compound the sites 8j and 8i were found to contain silicon fractions in the order of 10%. The refined atom positions at low temperatures are given in Table 1 (values in brackets), shifted by (1/4, 1/4, 1/4) for reasons given below. The resultant Rietveld fits of all compounds showed the presence of extra Bragg reflections of small intensity that were not indexed and fitted by the $ThMn_{12}$ structure model (Fig. 2a). These extra reflections can be described as superstructure reflections

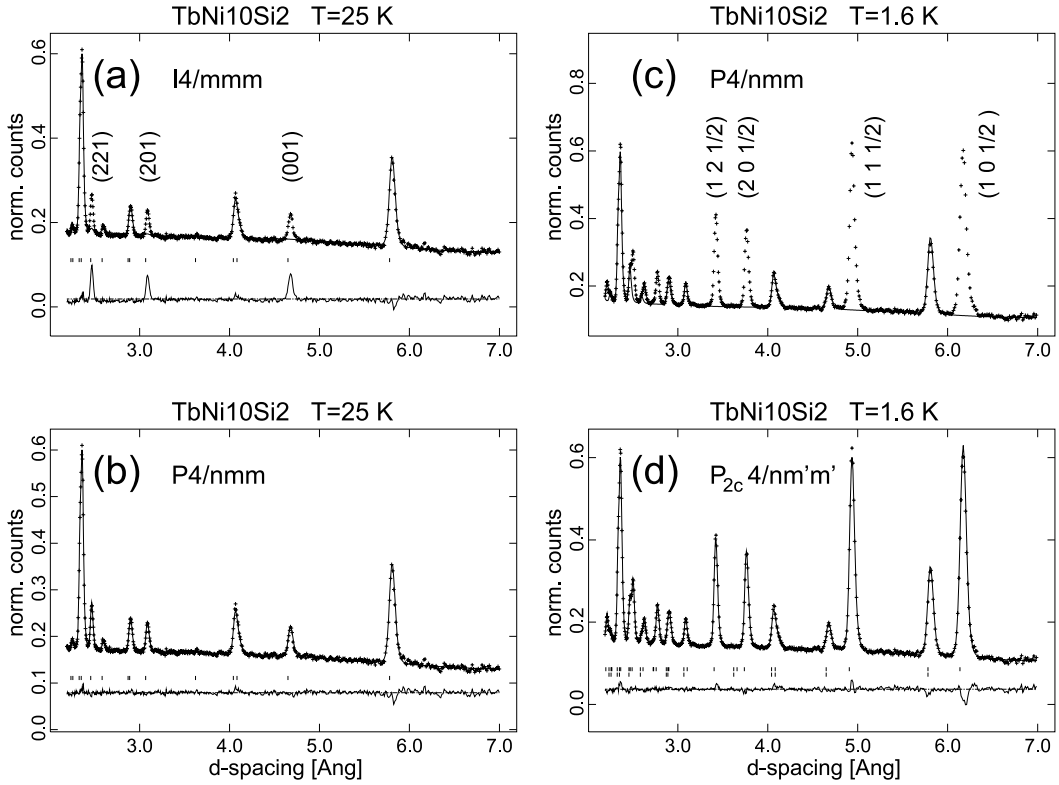

Fig. 2. Nuclear and magnetic superstructure reflections in sections of $TbNi_{10}Si_2$ diffraction patterns: (a) paramagnetic regime at 25 K, crystal structure fit in I4/mmm; (b) paramagnetic regime at 25 K, crystal structure fit in P4/nmm; (c) antiferromagnetic regime at 1.6 K, crystal structure fit in P4/nmm; (d) antiferromagnetic regime at 1.6 K, crystal structure fit in P4/nmm, magnetic fit in $P_{2c}4/nm'm'$.

and indexed with a modulation vector [0, 0, 1]. In other words the extra reflections can be indexed on the basis of the same tetragonal $ThMn_{12}$ unit cell by ignoring the reflection condition $h + k + l = 2n$ for the body centred lattice. It is important to note that the superstructure reflections were observed in the whole observed temperature range up to 300 K.

Space group P4/nmm (no 129), a maximal non-isomorphic 'klassengleiche' (k2) subgroup of the $ThMn_{12}$ space group I4/mmm, allows for the separation of the 8f site (I4/mmm) into two sites 4d and 4e (P4/nmm), for obtaining ordered distributions of Ni and Si. The second refinement model for the $RNi_{10}Si_2$ compounds was set-up in the second setting of P4/nmm. There is the following correspondence of crystallographic positions in P4/nmm $\leftrightarrow$ I4/mmm: 2c $\leftrightarrow$ 2a, 8f $\leftrightarrow$ 4d + 4e, 8i $\leftrightarrow$ 8i, 8j $\leftrightarrow$ 8i. Crystal structure starting parameters were taken from the I4/mmm model calculations by placing R on 2c(1/4,1/4, 0.25), Ni1 on 4d(0, 0, 0), Si on 4e(0, 0, 1/2), Ni2 on 8i(1/4, 0.6, 0.25) and Ni3 on 8i(1/4, 0.025, 0.75), taken into account a shift of the origin of the unit cell by (1/4, 1/4, 1/4). The refinements showed that the superstructure intensities could be explained by separating Ni and Si on 4d and 4e sites and by varying the z coordinates of the atoms. The refined structural parameters of $RNi_{10}Si_2$ compounds at low temperatures are summarised in Table 1. Table 1 contains the shortest interatomic distances R-X of atom positions to the rare earth atoms, and the position parameters and distances are compared to those obtained on the basis of the I4/mmm reference structure model.

The P4/nmm model could account for all observed peak positions and superstructure intensities of the five investigated compounds. Refinements of the occupancies revealed almost perfectly ordered crystal structures for all compounds, as displayed in Figure 1b: the rare earth atoms occupy the site 2c, Si exclusively occupies 4e, whereas the Ni atoms are located on the 4d and the two non-equivalent 8i positions. Figure 2b shows a section of the diffraction pattern fit of $TbNi_{10}Si_2$ at 25 K. Observed and calculated diffraction patterns of $DyNi_{10}Si_2$ and $HoNi_{10}Si_2$, $ErNi_{10}Si_2$, and $TmNi_{10}Si_2$ are displayed in Figure 3. The refinements of the occupancies led to following deviations from a full silicon occupation of site 4e: 1% for R = Tb, 4.5% for R = Dy, 3.7% for R = Ho, 2.7% for R = Er, and 1.6% for R = Tm, the values being within the 3σ limits of the estimated standard deviations of the least-squares refinements. That is to say there is an almost complete 1:1 atomic order of Ni and Si on 4d and 4e, respectively, observed in the whole temperature range up to ambient temperatures. This element order is a main characteristic of the crystal structure of the examined $RNi_{10}Si_2$ compounds. We conclude that $RNi_{10}Si_2$

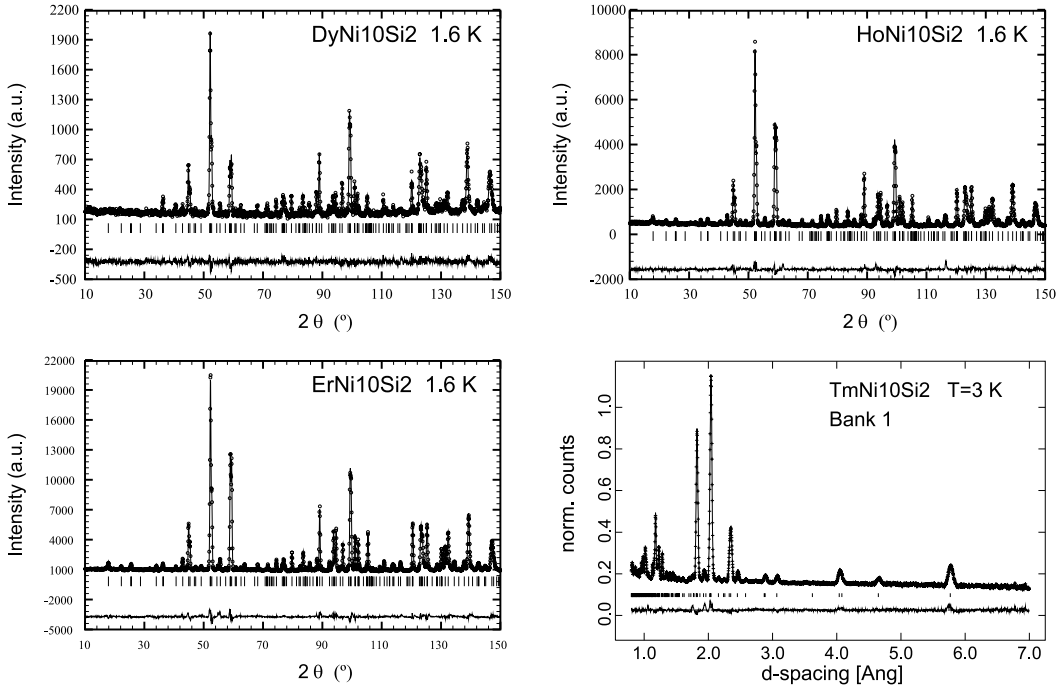

Fig. 3. Observed, calculated and difference angle-dispersive diffraction patterns of $DyNi_{10}Si_2$, $HoNi_{10}Si_2$ and $ErNi_{10}Si_2$ at 1.6 K; TOF diffraction pattern of $TmNi_{10}Si_2$ at 3 K.

compounds crystallize in an ordered structure variant of the $ThMn_{12}$ structure.

Atom sheets with R/Ni2/Ni3 perpendicular to the c-direction are separated by alternating Ni1 and Si-planes, in compliance with a modulation vector [0, 0, 1]. Atom positions and interatomic distances within the R/Ni2/Ni3 planes remain unchanged with respect to the $ThMn_{12}$ average structure. There are, however, distinct atom shifts of R, Ni2 and Ni3 atoms along the c-direction, away from the special positions of the I4/mmm parent structure, as is evident from the z-coordinates (Tab. 1). The R atom displacements from $z = 1/4$ are such that R atoms have the largest possible distances R-X to the silicon atoms. It is worth noting that the Rietveld refinements based on the $ThMn_{12}$ structure model showed a preferred silicon occupation of the 8f positions which also have largest distances to the rare earth atoms. Considering that the lower symmetry structure of $RNi_{10}Si_2$ with respect to $ThMn_{12}$ allows silicon atoms to occupy positions even further away from the rare earth atoms (*e.g.* 3.1684 Å instead of 3.1242 Å for Tb-Si in $TbNi_{10}Si_2$), it is worth mentioning that some of the Si-Ni interatomic distances become shorter (*e.g.* 2.322 Å instead of 2.367 Å for Si-Ni3 in $TbNi_{10}Si_2$). The displacement of R atoms from the centre of the 8f = 4d + 4e tetragonal prism away from the Si layers may be just due to the larger atom size of Si (atom radius 1.32 Å) compared to Ni (1.25 Å) [18].

The 1:1 site separation of Si and Ni atoms on the 8f site of the $ThMn_{12}$ structure probably just reflects the symmetry principle that atoms of the same sort tend to occupy symmetry equivalent positions. It is surprising, however, that the lower symmetry structure P4/nmm has not so far been reported for other $RT_{10}M_2$. The formation of a perfect elemental order may be strongly dependent on the preparation conditions. A case for observed site preferences in other $ThMn_{12}$ rare earth silicides is often made in terms of the atomic radii and the heat of mixing of the rare earth elements and silicon [3]. Nearest neighbour distances in $RNi_{10}Si_2$ pose similar steric constraints as in other $ThMn_{12}$ compounds, for example $RFe_{12-x}M_x$ [19], in that the 8i site offers more space than the 8f site to accommodate bigger atoms like Si compared to Ni. The neutron data showed that Si avoids the site 8i, *i.e.* atom size effects apparently play a minor role. From the point of view of the R-Si mixing enthalpy, Si would favour the sites 8f and 8j. According to the neutron diffraction data, however, the Si atoms avoid the 8j site as well as the 8i site. We conclude that atom size and R-Si enthalpy effects cannot explain the preferred site distribution of Si satisfactorily on their own.

3.2 The magnetic ordering behaviour

The compounds with R=Dy, Er, Ho, and Tm do not display any magnetic Bragg intensities down to temperatures of 1.6 K and 3.0 K, respectively. The neutron diffraction patterns of $TbNi_{10}Si_2$, however, reveal new superstructure reflections as the sample is cooled down from 25 to 1.6 K. Figure 2c shows that the peak positions of the magnetic Bragg reflections of $TbNi_{10}Si_2$ at 1.6 K are incompatible with the P4/nmm crystal structure unit cell. The magnetic reflections are superstructure peaks that can be indexed with a commensurate propagation vector of [0, 0, 1/2], *i.e.* involves a cell doubling of the chemical

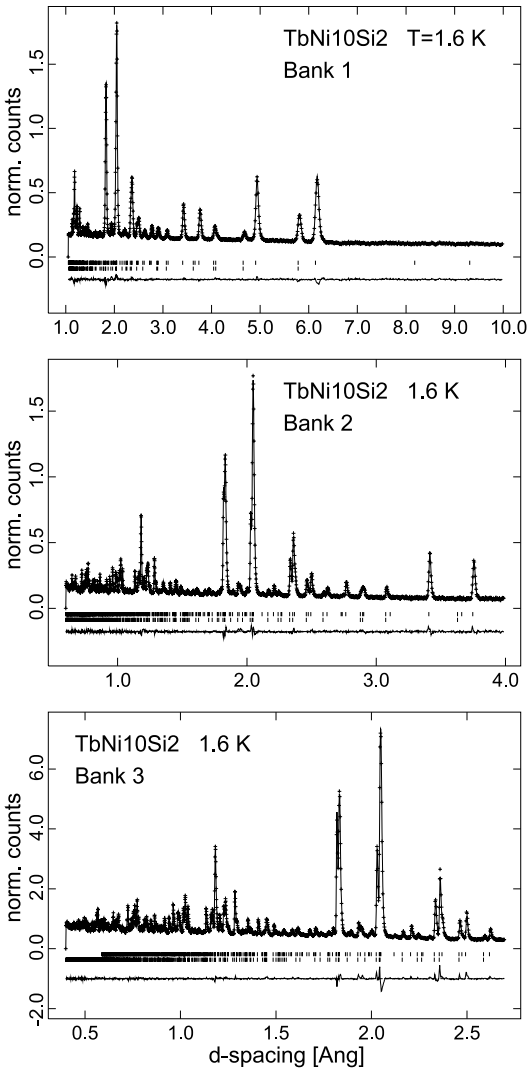

Fig. 4. Observed, calculated and difference TOF diffraction patterns of $TbNi_{10}Si_2$ at 1.6 K obtained from three ROTAX detector banks. Upper row of reflection markers indicate peak positions with respect to the doubled magnetic cell $A = a$, $C = 2c$. Lower row of reflection markers indicate reflection positions with respect to the crystallographic cell and space group P4/nmm.

cell along the c-axis. The magnetic reflections in Figure 2c are indexed according to $(H, K, L) = (h, k, l) \pm (0, 0, 1/2)$ where (H, K, L) and (h, k, l) denote magnetic and nuclear peaks, respectively.

For the magnetic model set-up it is important to note that magnetic Bragg intensities are absent at $(0, 0, L)$-peak positions, in particular, there is no Bragg peak at the (0, 0, 1/2) position at 9.3 Å (Fig. 4). This reflection extinction of $(0, 0, L)$-peaks is related to the magnetic moment directions parallel to the c-axis of the magnetic unit cell according to

$$I_M \propto \sin^2 \alpha |F_M|^2 \quad (1)$$

where I_M is the magnetic Bragg intensity, alpha is the angle between the scattering vector and the magnetic moment, and F_M is a structure factor for collinear magnetic structures [20]. Magnetic structure models allowed for both ordering of magnetic Tb moments on the 2c site and induced magnetic order on the Ni sites 4a and 8i. The 2c site symmetry, 4mm, leads to an admissible magnetic site symmetry 4m′m′ for the Tb atoms [21] restricting the terbium moments $m_{\mathrm{Tb}} = (0, 0, m_z)$ to directions parallel to the tetragonal c-axis, in agreement with the $(0, 0, L)$ extinction observation. The magnetic space group $P_{2c}4/nm'm'$, derived from the crystal structure space group P4/nmm [21], accounts for the magnetic site symmetry and the cell doubling along the c-axis. The magnetic symmetries restrict the magnetic moment vectors on the Ni sites 2a and 8i to $m_{\mathrm{Ni}} = (m_x, m_x, m_z)$ but only m_z-components of Ni moments were taken into consideration in accordance with the absence of $(0, 0, L)$ reflections. The magnetic moment refinements of $TbNi_{10}Si_2$ were performed with the program GSAS by introducing a purely magnetic phase with a unit cell $A = a$, $C = 2c$ with respect to the lattice parameters a, c of the crystallographic cell. A magnetic form factor of Tb^{3+} was used as derived from $f = \langle j0 \rangle + c\langle j2 \rangle$ with $c(Tb^{3+})$ calculated using the dipole approximation [22]. The form factor of Ni was calculated using the $\langle j0 \rangle$ form factor only. Coefficients A_i, B_i of the $\langle j0 \rangle$ and $\langle j2 \rangle$ form factor expansions, as implemented in the GSAS program, were taken from the International Tables for Crystallography [23].

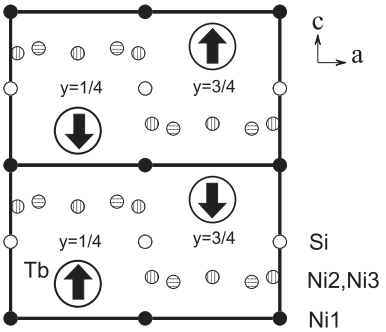

Fig. 5. Magnetic structure of $TbNi_{10}Si_2$, space group $P_{2c}4/nm'm'$.

The refinements showed that the Ni sites of $TbNi_{10}Si_2$ do not carry magnetic moments and that the magnetic intensities can be accounted for by long-range order on the Tb site alone. The refined fully ordered Tb moment at 1.6 K is 8.97(2) μ_{B}. The upper limit for Ni moments on the three Ni sites was determined to be 0.2 μ_{B}. The best Rietveld fits for $TbNi_{10}Si_2$ at 1.6 K are shown in Figure 4. The magnetic propagation vector fully describes the phases between the magnetic terbium moments, *i.e.* the sequence up-down-down-up of Tb moments along the c-direction as displayed in Figure 5, in agreement with the magnetic space group $P_{2c}4/nm'm'$. Nearest Tb neighbours, separated by the c-lattice parameter distance, are coupled antiferromagnetically. The magnetic structure solution for $TbNi_{10}Si_2$ is unique, there is no loss of information due to powder or domain averaging. It is worth noting that a magnetic propagation of [0, 0, 1/2] has never

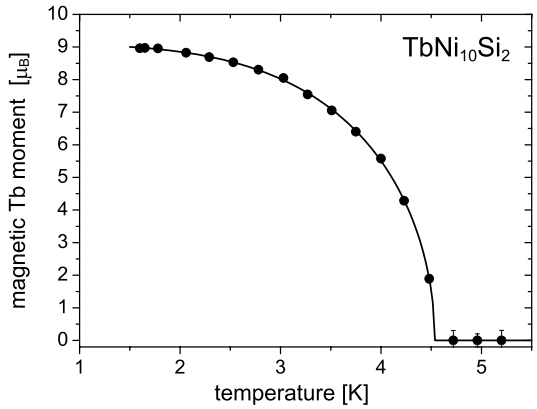

Fig. 6. Temperature dependence of the ordered Tb moment in $TbNi_{10}Si_2$. Points mark refined moment values, the solid line represents a power-law fit.

been observed for $ThMn_{12}$ compounds, as far as we know. Also, there is no magnetic space group for I4/mmm that involves a cell doubling along the *c*-axis [21], that is to say crystallization in the lower symmetry P4/nmm group prepares for the observed magnetic structure of $TbNi_{10}Si_2$.

The temperature variation of the terbium moments is displayed in Figure 6. The neutron diffraction data do not indicate a change of the type of antiferromagnetic structure in the temperature range of magnetic order. The magnetic structure remains commensurate as the temperature is increased towards the transition temperature. The magnetic moment values were used to fit the phenomenological formula [24]

$$m_{\mathrm{Tb}}(T) = K\,[1 - (T/T_N)^e]^\beta \qquad (2)$$

where K is a scaling constant. The fit parameters for $TbNi_{10}Si_2$ are: Néel temperature $T_N = 4.53(1)$ K, exponents $e = 3.7(1)$ and $\beta = 0.50(2)$. The temperature dependence of the Tb moment signifies a second order phase transition. For T close to T_N the fit parameter $\beta = 0.5$ can be associated with the critical exponent of the phase transition and indicates classical mean field behaviour.

The refined magnetic Tb moment is close to maximum possible ordered moment $gJ\mu_B = 9\mu_B$, where g is the Landé factor and J is the total angular momentum of the ground state of the free ion Tb^{3+}. This suggest that there is no structural frustration that hampers the ordering process. This observation may also imply that the RKKY exchange interaction is very strong compared to the crystal field interaction [25], although this appears to be implausible because the crystal field levels in $RNi_{10}Si_2$ compounds typically spread over about 70 K [13]. Another possibility to forming the full moment is at least one low-lying $|J_z = \pm 6\rangle$ level of the $J = 6$ multiplet of Tb^{3+} at an energy comparable to the exchange energy above the ground state. With RKKY as the magnetic coupling mechanism for the isostructural $RNi_{10}Si_2$ compounds the transition temperatures are expected to scale with the de Gennes factor $(g-1)^2 J(J+1)$ [25], hence the transition temperatures for R = Dy, Ho, Er, Tm would be expected to be below $T_N = 4.5$ K of the Tb compound. In fact, the Curie temperatures of the compounds $RFe_{10}Si_2$ linearly increase with the de Gennes factor [2]. Assumption of a linear de Gennes type behaviour for the rare earth nickel silicides and normalisation to the Néel temperature of $TbNi_{10}Si_2$ lead to transition temperatures of about 3.0, 1.5, 1.0, and 0.5 K for the Dy, Ho, Er and Tm compounds, respectively. This confirms the absence of long range magnetic order as low as 1.6 K for $HoNi_{10}Si_2$, $ErNi_{10}Si_2$, and $TmNi_{10}Si_2$. The absence of a magnetic phase transition of $DyNi_{10}Si_2$ at 3 K, on the other hand, implies that the transitions temperatures do not linearly increase with the de Gennes factor.

4 Conclusions

We report on the crystal and magnetic structures of $RNi_{10}Si_2$ compounds studied by neutron diffraction. To our knowledge, this is the first time that an ordered structure variant is found in the important class of $ThMn_{12}$ compounds. The space group P4/nmm is a maximal subgroup of I4/mmm thus allowing for the possibility of a continuous second order phase transition from the ordered Ni/Si distributions, as observed, towards a disordered phase above room temperature. In the covered temperature range down to 1.6 K only $TbNi_{10}Si_2$ orders magnetically. A Néel temperature of 3 K for the Dy compound, as suggested by the Gennes scaling of transition temperatures, is not confirmed but it can be assumed that all compounds with R = Dy, Ho, Er, Tm order magnetically below 1.6 K. The Tb antiferromagnetic order of $TbNi_{10}Si_2$ with [0, 0, 1/2] is unusual for $ThMn_{12}$ compounds. The magnetic structure develops a fully ordered moment at 1.6 K and a β exponent of 0.5. Thus, $TbNi_{10}Si_2$ behaves very much like an ideal classical mean field system. This rather simple and classic magnetic order of Tb moments on the 2c site may well reflect the absence of structural disorder in the series $RNi_{10}Si_2$, a disorder that is intrinsically present in the many other $ThMn_{12}$ compounds due to element mixing on equivalent symmetry positions.

The authors gratefully acknowledge provision of neutron beam time by ISIS, BENSC, and ANSTO. Financial support of one of us (W.K.) and ROTAX under the project 03KLE8BN by the German BMBF is gratefully acknowledged .

References

1. K.H.J. Buschow, J. Magn. Magn. Mater. **100**, 79 (1991)
2. J.J.M. Franse, R.J. Radwanski, in *Rare-earth iron permanent magnets*, edited by J.M.D. Coey (Clarendon Press, Oxford, 1996), p. 143
3. K.H.J. Buschow, J. Appl. Phys. **63**, 3130 (1988)
4. H. Tang, E. Brück, F.R. de Boer, K.H.J. Buschow, J. Alloys, Comp. **243**, 85 (1996)
5. H. Tang, G.W. Qiao, J.P. Liu, D.J. Sellmyer, F.R. de Boer, K.H.J. Buschow, Solid State Comm. **117**, 565 (2001)

6. J.V. Florio, R.E. Rundle, A.I. Snow, Acta Cryst. **5**, 449 (1952)
7. P. Schobinger-Papamantellos, K.H.J. Buschow, I.H. Hagmusa, F.R. de Boer, C. Ritter, F. Fauth, J. Magn. Magn. Mater. **202**, 410 (1999)
8. W. Schäfer, W. Kockelmann, I. Halevy, J. Gal, Mater. Sci. Forum **321-324**, 670 (2000)
9. W. Schäfer, W. Kockelmann, G. Will, P. Fischer, J. Gal, J. Alloys, Comp. **207/208**, 316 (1994)
10. J.A. Paixão, M. Ramos Silva, S.Aa. Sorensen, B. Lebech, G.H. Lander, P.J. Brown, S. Langridge, E. Talik, A.P. Gonçalves, Phys. Rev. **61**, 6176 (2000)
11. A. Chełkowski, E. Talik, J. Szade, J. Heimann, A. Winiarska, A Winiarski, Physica B **168**, 149 (1991)
12. O. Moze, R.M. Ibberson, K.H.J. Buschow, Solid State Comm. **78**, 473 (1991)
13. O. Moze, R. Caciuffo, K.H.J. Buschow, G. Amoretti, J. Magn. Magn. Mater. **104-107**, 1391 (1992)
14. P. Stefanski, W. Suski, K. Wochowski, T. Mydlarz, Solid State Comm. **97**, 465 (1996)
15. J. Rodriguez-Carvajal, Physica B **192**, 55 (1993); FullProf version wfp2k
16. A.C. Larson, R.B. Von Dreele, *General Structure Analysis System (GSAS)*, Los Alamos National Laboratory Report LAUR 86-748 (1994)
17. V.F. Sears, Neutrons News **3**, 29 (1992)
18. W.B. Pearson, *The crystal chemistry and physics of metals and alloys* (Wiley-Interscience, New York, London, Sydney, Toronto, 1972), p. 150
19. L. Wang, N. Tang, Y.P. Shen, D. Yang, B. Fuquan, G.H. Wu, F.M. Yang, F.R. de Boer, E. Brück, K.H.J. Buschow, J. Appl. Phys. **91**, 2165 (2002)
20. J. Rossat Mignod, Magnetic structures, in Methods of experimental physics, edited by K. Sköld, D.L. Price (Academic Press, Orlando, San Diego, New York, Austin, Boston, London, Sydney, Tokyo, Toronto, 1987), p. 69
21. W. Opechowski, R. Guccione, *Magnetic Symmetry*, in *Magnetism*, Vol. IIA, edited by G.T. Rado, H. Suhl (Academic Press, Yew York, 1963), p. 105
22. D.F. Johnston, Proc. Phys. Soc. **88**, 87 (1966)
23. P.J. Brown, *Magnetic form factors*, in *International Tables for Crystallography*, Vol. C, edited by A.J.C. Wilson (Kluwer Academic Publishers, Dordrecht, Boston, London, 1995), p. 391
24. K. Hagedorn, D. Hohlwein, J. Ihringer, K. Knorr, W. Prandl, H. Ritter, H. Schmid, Th. Zeiske, Eur. Phys. J. B **11**, 243 (1999)
25. A. Szytula, J. Leciejewicz, *Handbook of crystal structures and magnetic properties of rare earth intermetallics* (CRC Press, Boca Raton, Ann Arbor, London, Tokyo 1994), p. 63